

Synthesis, Characterization, and cytotoxicity of FeCO₃ nanoparticles on the HL-60 human leukemia cell line

Ragdaa Majeed¹ , Mustafa Hammadi²

Abstract

In medicine, nanoparticles are successfully replacing anticancer drugs (NPs). In this study, FeCO₃-NPs were produced using the co-precipitation method (A), while the green chemistry method and turmeric extract were employed in the latter (B). Several methods were characterized, including FTIR, XRD, EDX, and SEM. The average size of FeCO₃-NPs (A) and FeCO₃-NPs (B) particles in the XRD was 26.96 nm and 30.60 nm, respectively. According to EDX, the synthesized NPs have a high degree of purity. FeCO₃-NPs (A) were evaluated on HL-60 cells at 25, 50, 100, 200, and 400 µg/ml dosages. Following 24 hours, the killing rate was, in descending order, 39.4%, 61.64%, 78.14%, 91.44%, and 66.344%. And in that sequence, the death rate of ZnCO₃-NPs (B) was 18.4%, 28.6%, 42.2 %, 52.5 %, and 80.6 %. Chemical precipitation is a better method for killing or inhibiting. Half-maximal inhibitory doses (IC₅₀) for FeCO₃-NPs for A and B are 34.98 and 135.2 µg/ml, respectively. FeCO₃-NPs have potential therapeutic advantages as anticancer drugs. The drug was safe at all concentrations (not harmful).

Keywords: FeCO₃-NPs, co-precipitation, Turmeric, Cytotoxicity, HL-60

التوليف والتوصيف والسمية الخلوية لجسيمات FeCO₃ النانوية على خط خلايا سرطان الدم البشري
HL-60

رغداء عبد اللطيف مجيد¹ ، أ.د. مصطفى عبد المجيد حميد²

المستخلص

في الطب، تحل الجسيمات النانوية محل الأدوية المضادة للسرطان (NPs) بنجاح. في هذه الدراسة، تم إنتاج FeCO₃-NPs باستخدام طريقة الترسيب المشترك (A)، بينما تم استخدام طريقة الكيمياء الخضراء ومستخلص الكركم في الأخير (B) تم تمييز عدة طرق، بما في ذلك FTIR و XRD و EDX و SEM. متوسط حجم جزيئات FeCO₃-NPs (A) و FeCO₃-NPs (B) في XRD 26.96 نانومتر و 30.60 نانومتر، على التوالي. وفقاً لـ EDX، تتمتع NPs المركبة بدرجة عالية من النقاء. تم تقييم FeCO₃-NPs (A) على خلايا HL-60 بجرعات 25 و 50 و 100 و 200 و 400 ميكروغرام / مل. بعد 24 ساعة، كان معدل القتل، بترتيب تنازلي، 39.4%، 61.64%، 78.14%، 91.44%، و 66.344%. وفي هذا التسلسل، كان معدل الوفيات من ZnCO₃-NPs (B) 18.4% و 28.6% و 42.2% و 52.5% و 80.6%. يعتبر الترسيب الكيميائي طريقة أفضل للقتل أو التثبيط. الجرعات المثبطة نصف القصوى (IC₅₀-FeCO₃-NPs) هي 34.98 و 135.2 ميكروغرام / مل على التوالي. FeCO₃-NPs لها مزايا علاجية محتملة مثل الأدوية المضادة للسرطان. كان الدواء آمناً بجميع التركيزات (غير ضار).

الكلمات المفتاحية: FeCO₃-NPs، الترسيب المشترك، الكركم، السمية الخلوية، HL-60

Affiliation of Authors

^{1,2} College Education for Pure Science, Univ Diyala, Iraq, Diyala, 32001

¹ Ragdaamajeed@gmail.com

² mustafa.hameed@uodiyala.edu.iq

¹ Corresponding Author

Paper Info.

Published: Jun. 2025

انتساب الباحثين

^{1,2} كلية التربية للعلوم الصرفة، جامعة ديالى، العراق، ديالى، 32001

¹ Ragdaamajeed@gmail.com

² mustafa.hameed@uodiyala.edu.iq

¹ المؤلف المراسل

معلومات البحث

تاريخ النشر: حزيران 2025

Introduction

One of the hematologic malignancies that affect the bone marrow, lymphatic system, and blood cells the most frequently in adults is leukemia [1]. Leukemia is identified by the unchecked.

Production of poorly differentiated white blood cells and clonal hematopoiesis occurs in the bone marrow. The type of leukemia, age, the severity of the disease, and the patient's medical history all

affect how this disease is treated. Patients typically receive targeted chemotherapy, radiation therapy, and bone marrow transplants as part of their treatment plans [2]. There are numerous distinct forms of leukemia. Leukemia is usually categorized into acute and chronic leukemias based on how quickly it develops. Leukemia is primarily categorized into lymphoid and myeloid leukemias based on the types of cells present [3]. Deliver therapeutic medications effectively, improve targeting, and achieve controlled release. Nanotechnology for medicine delivery has recently been created. Through intelligent design, nanoparticles could overcome the drawbacks of conventional medicine and enable the creation of individualized delivery platforms that incorporate diagnostic, treatment, and other functions [4,5]. Nanoscale materials are used for illness detection or precisely focused drug administration in nanomedicine, a young but developing field of study. One of the best uses of nanomedicine is the targeted administration of chemotherapeutic, immunotherapeutic, and biologic medicines to treat various diseases [6]. Therapeutics based on nanoparticles can potentially change how different human diseases are treated. However, nanoparticle instability and early release reduce medication bioavailability, which hinders clinical translation. Minor alterations may result in significant changes to the Nano formulation because all nanoparticles must rely on control at the nano-size scale [7]. Human cancer risk has been compared with iron consumption, iron metabolism, and iron metabolism in population-based research. High body iron levels and cancer have been linked in several studies, but not all of them, as summarized in [8,9]. Metals like iron are necessary for biological functions. Iron is a crucial inorganic nutrient for the human body and is necessary for

oxygen delivery, ATP creation, DNA synthesis, and repair [10,11]. The study of iron biology, especially its cancer-related components. Novel cancer therapeutic strategies that entail iron disturbances have been proposed, and links between iron and cancer have been identified. The understanding of iron trafficking has advanced significantly over the past ten years, incorporating previously unrecognized processes of absorption and efflux as well as intracellular and intercellular iron redistribution that affects tumor behavior and medication response. Additionally, iron is now understood to affect both tumor growth and the likelihood of metastasis. Iron has also been acknowledged as a crucial component in ferroptosis, the named mechanism of cell death that may eventually allow us to target the iron addiction of cancer cells, in contrast to these pro-tumorigenic actions. We have concentrated on current findings of molecules and pathways that connect iron homeostasis and cancer in order to explore these subjects properly. To complete the picture of iron dysregulation and cancer, we direct the reader to additional reviews that discuss population-based studies, the function of mitochondrial iron, and early experimental research on the connection between iron and cancer [12].

Synthesis of FeCO₃ Nanoparticles by Co-Precipitation

FeCl₃·6H₂O and Na₂CO₃ were combined in an amount of 0.5 M, and the mixture was stirred on a magnetic stirrer for six hours at 50 °C. A pH adjustment of 7 was made. The filtrate was then filtered and dried at 120 °C for four hours.

Synthesis of FeCO₃ Nanoparticles by green chemistry

A mixture of 100 g of turmeric was taken, and 1L deionized water was added and placed on the magnetic stirrer for two hours at a temperature of 50 °C, then left in a dark place for 24 hours. Then the mixture was filtered, and the extract was used in the preparation of FeCO₃ Nanoparticles by FeCl₃.6H₂O and Na₂CO₃ were combined in an amount of 0.5 M, and the mixture was stirred on a magnetic stirrer for six hours at 50 °C. A pH adjustment of 7 was made. The filtrate was then filtered and dried at 120 °C for four hours.

Approaches for characterization

Numerous techniques, such as X-ray diffraction (XRD), Fourier-transform infrared (FTIR) spectroscopy, and scanning electron microscopy (SEM), were used to analyze the FeCO₃ nanoparticles (SEM). XRD was used to determine the crystallite size of the nanoparticles (Shimadzu, Kyoto, Japan). The samples' FTIR spectra were obtained using a Shimadzu (Tokyo, Japan). SEM analysis was performed using a 200 kV Zeiss SEM (Germany).

FeCO₃ nanoparticle MTT assay

MTT dye (3-[4,5-dimethylthiazole-2-yl]-2,5-diphenyltetrazolium bromide) (10 mg/ml) was used for this experiment. Samples of FeCO₃ nanoparticles were dissolved in 0.2 % DMSO to obtain concentration gradients of 25, 50, 100, 200, and 400 µg/ml. A sample of 200 µl of suspended cells (1 × 10⁴ cells/well) prepared in RPMI media was disseminated. The cells were cultured at 37 °C for 24 hours with 5% CO₂. The cell cultures were then incubated for an additional 24 hours under the same circumstances after receiving 20 µl of

FeCO₃-NPs treatment. Each sample was then given 10 µl of MTT reagent, which was then incubated for 5 hours at 37°C. At 570 nm, the absorbance was measured [13].

Hemolysis assay for FeCO₃ nanoparticle

To find toxic or non-toxic chemicals, the hemolysis assay was employed to screen for FeCO₃ at different doses (50, 200, and 400 µg/ml). After being taken from the lab and placed in an (EDTA) tube, the blood sample was analyzed on a slide and examined under a microscope at a magnification of (100). The blood cells and plasma were separated using an (EDTA) tube and placed in a centrifuge for 10 minutes. After removing the plasma layer from the cells, the cells were repeatedly washed with PBS, each time adding 1ML of PBS, and the centrifuge cycle was repeated for 10 minutes. After two minutes, the cells were withdrawn from the PBS. After the blood cells had been washed multiple times, the blood cell suspension was created by combining (1ML) with (9ML) PBS. The antagonist is added to each tube with a volume of (1200 µL) in varying concentrations, and (300 µL) of the cell suspension is added to the final volume (1.5 ml). Each tube is then incubated in the incubator for two hours before being spun apart at a rate of 1000 cycles per minute for five minutes. The Heh control parameters were then used to measure the difference in hemolysis (test tube containing blood and deionized water only, test tube containing blood and PBS). After centrifugation, the (+) option displays the compound's toxicity when mixed with blood components. The fact that the blood components were not combined after centrifugation, as shown by the (-) option, suggests that the drug was not harmful [14].

Results and discussion

Characterization of FeCO₃ nanoparticles by FTIR

FeCO₃ prepared by co-chemical precipitation A was diagnosed by FT-RT as shown in Figure 1. The appearance of a weak band at the frequency (462.92 cm⁻¹) due to the stretching of the (Fe-O) U and a sharp and medium at the site (1080.14cm⁻¹) due to the frequency of the (C-O) U, as we notice a band medium and wide and broad at a frequency (1589.34cm⁻¹) due to the stretching of the (C = O) bond and a comprehensive and broad at a

frequency (3387.00cm⁻¹) due to the stretching of the (O-H) bond. As for FeCO₃ prepared by green chemistry B, a weak band appears at the frequency (462.92cm⁻¹) due to the stretching of the bond. (Fe-O) U and a weak band in position (1064.71cm⁻¹) that goes back to the frequency of the band (C-O) U. We also notice a medium and wide band at the frequency (1527.62cm⁻¹) that goes back to the stretching of the band C=O U and a wide band at the frequency (3387.00cm⁻¹) that goes back to the stretching of the U(O-H) sphincter are consistent with the literature [15,16,17].

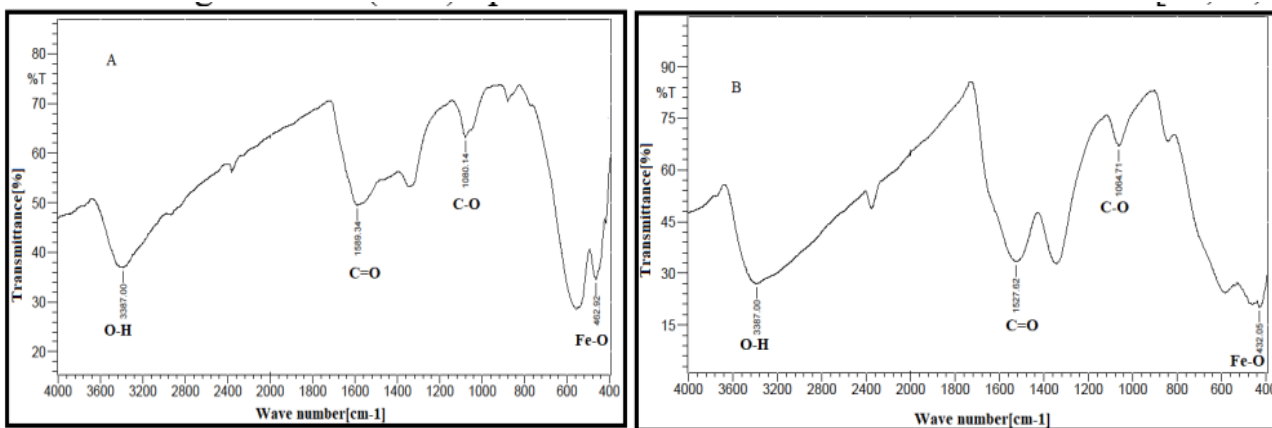


Figure (1): Characterization of FeCO₃ nanoparticles by FTIR

Characterization of FeCO₃ nanoparticles by X-ray diffraction

Using the International Center for XDR Database (ICDD), the FeCO₃ X-ray spectra were compared to the FeCO₃ standard spectrum in Figure (2).

Card number 01-075-1508 FeCO₃ nanoparticles produced using the chemical precipitation method A had an average crystal size of (26.96nm). FeCO₃ nanoparticles made using green chemistry B had an average crystal size of 30.60 nm.

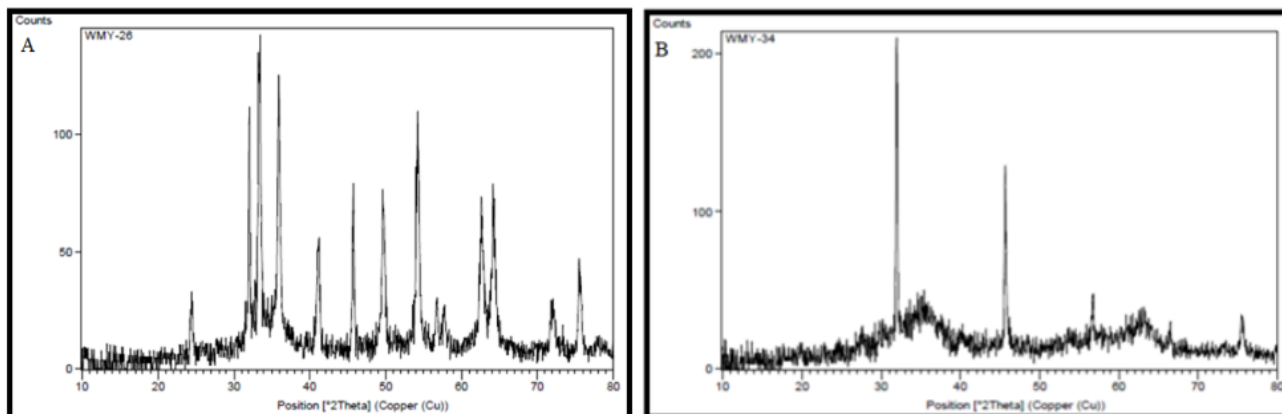


Figure (2): X-ray diffraction spectrum of FeCO₃nanoparticles

Characterization of FeCO₃ nanoparticles by energy-dispersive X-rays

The elements found in FeCO₃NPs were identified using energy-dispersive X-ray, as depicted in Figure 3. The results showed that iron, 57.8%, oxygen, 28.5%, and carbon, 11.8%, were present

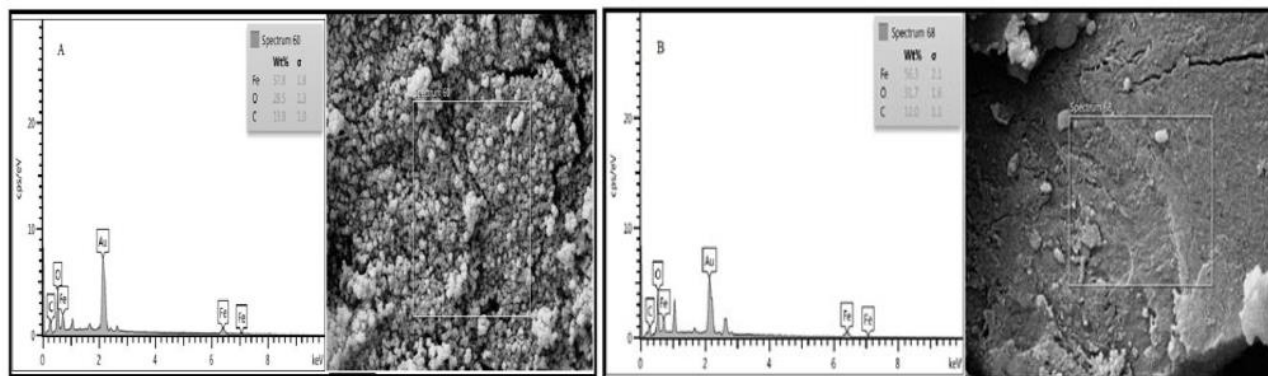


Figure (3): Energy-dispersive X-rays of FeCO₃nanoparticles

Characterization of FeCO₃nanoparticles by SEM

The morphological and structural makeup of FeCO₃NPs was studied using an SEM scanning electron microscope. The nanoparticles were

in sample A, demonstrating the high degree of purity of the zinc carbonate nanoparticles. The results from experiment B showed high levels of purity in the iron carbonate nanoparticles, with an iron content of 56.3%, oxygen at 31.7%, and carbon at 12.0%.

produced at the nanoscale level, and experiment A data from Figure 4 demonstrate that their average diameter is 72.638 nm. The diameter of the results from experiment B is 86.103 nm on average.

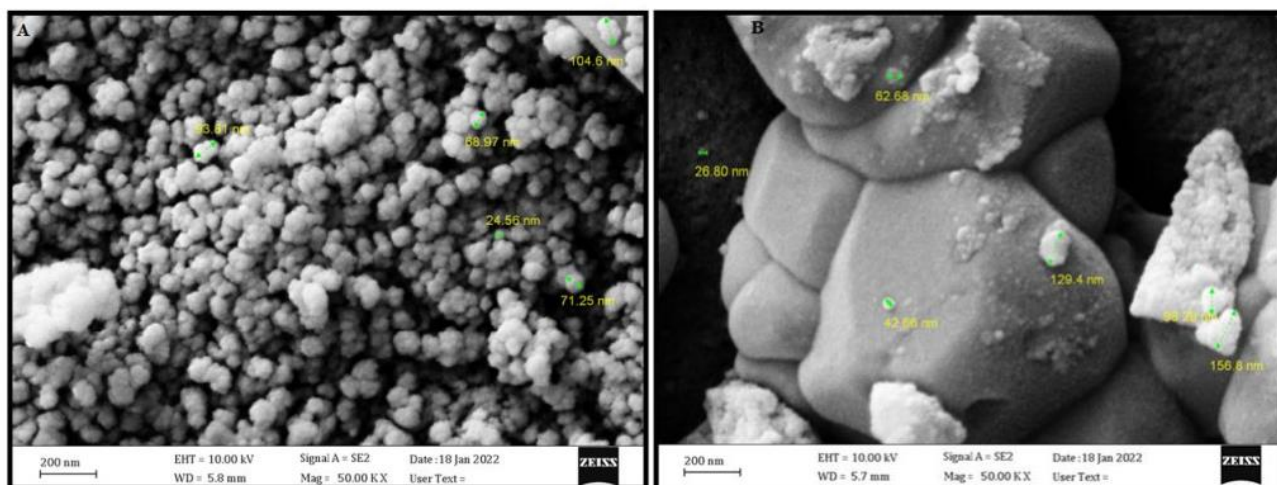


Figure (4): SEM of FeCO₃nanoparticles

Inhibition of FeCO₃ nanoparticles for HL-60 blood cancer cells

The results in Figure 5 showed the survival rate of HL-60 cells after adding the mixed FeCO₃ by the chemistry precipitation method A at different

concentrations (25-400 μg/ml) compared to Blank for 24 hours of incubation. At a concentration of 25, the killing rate was 39.4%, and at a concentration of 50, the killing rate was 61.6%. While at the concentration of 100, the killing rate was 78.1%, at the concentration of 200, the killing

rate was 91.4%, which indicates a relationship between the increase in the concentration and the percentage of inhibition or killing. At a concentration of 400, the killing rate is 95.8%. As for the FeCO_3 prepared using the green chemistry method B, at a concentration of 25, the killing rate was 18.4 percent, and at a concentration of 50, the

killing rate was 28.6%. While at the concentration of 100, the killing rate was 42.2%, at the concentration of 200, the killing rate was 52.5%. At the concentration of 400, the killing rate was 80.6%, which indicates that the FeCO_3 prepared by the chemical precipitation method is more effective in inhibiting or killing.

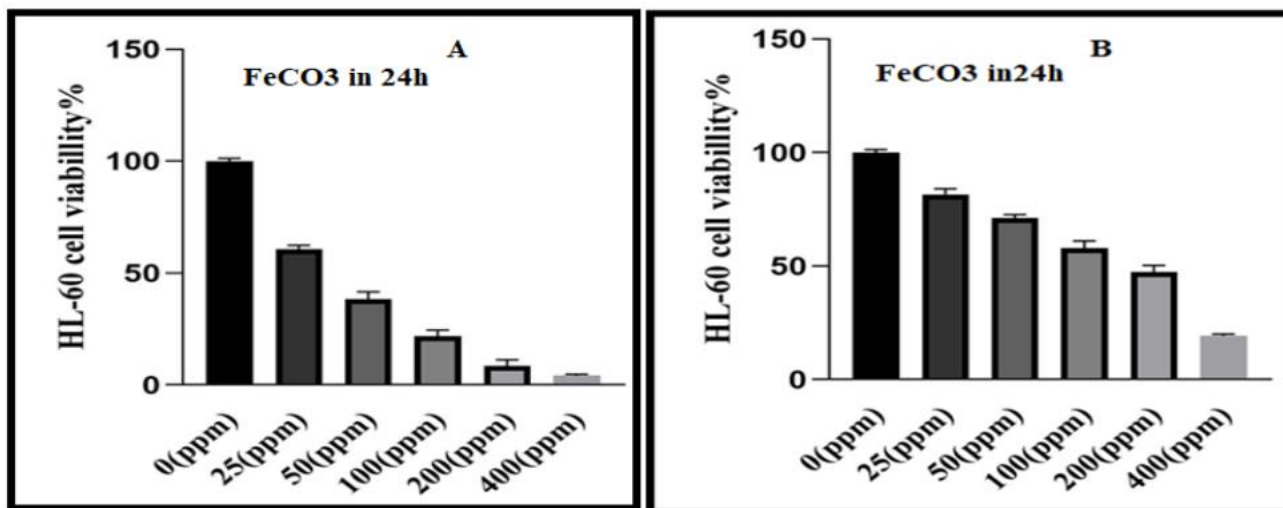


Figure (5): Inhibition of FeCO_3 nanoparticles for HL-60 in 24 h

After 24 hours of incubation with HL-60 blood cancer cells, the half-maximal inhibitory concentration (IC_{50}) of FeCO_3 nanoparticles via chemical precipitation A was assessed using a

normalized response. Fig. 6 depicts the IC_{50} value as $34.98\mu\text{g/ml}$. Using method B of green chemistry, FeCO_3 was created. A relatively low IC_{50} value was $135.2\mu\text{g/ml}$.

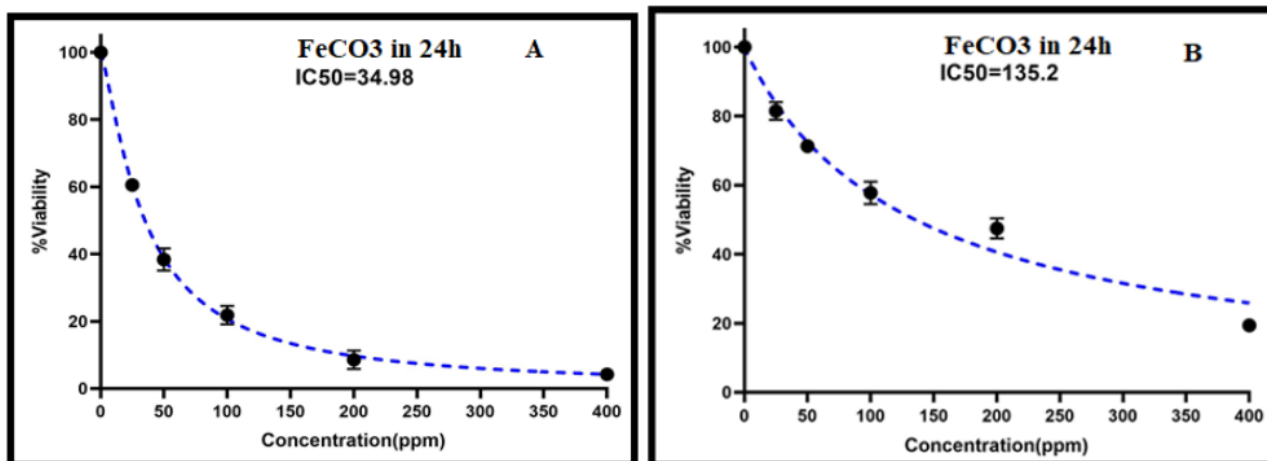


Figure (6): IC_{50} of FeCO_3 nanoparticles for HL-60 Blood cancer cells

Figure (7) shows the cytotoxicity of the compound of FeCO_3 nanoparticles via the chemical precipitation technique, A, investigated, and the

results showed that the compound was safe (non-toxic) at all concentrations, also, for method B of green chemistry.

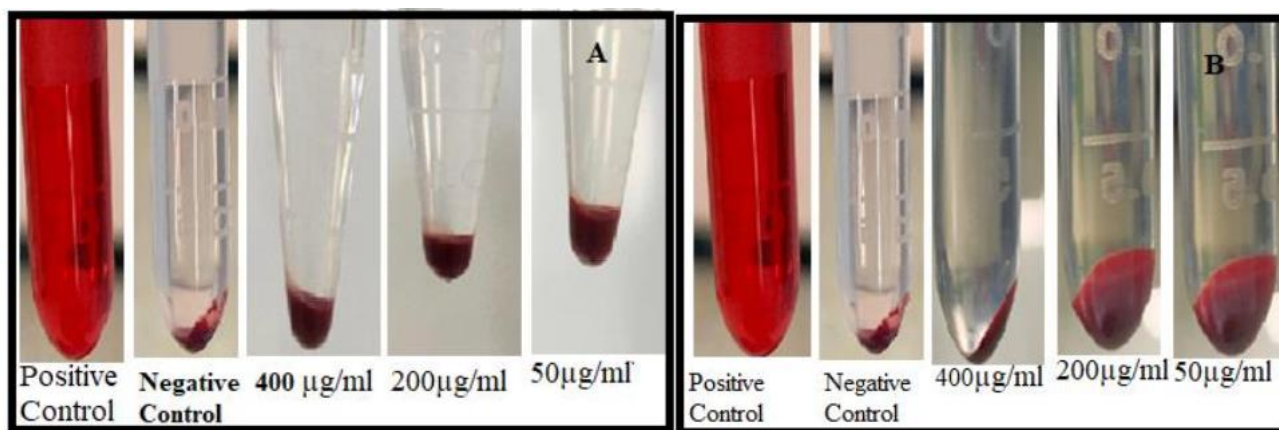


Fig. 7: Hemolysis test for FeCO₃ nanoparticles

In recent years, there has been a lot of interest in using nanoparticles to treat blood cancer. To create a practical nanotechnology method, metal nanoparticle creation and modification depend on the form, size, and target accumulation. FeCO₃ nanoparticles are among the nanoparticles that are promising in modern nanobiotechnology for various uses, including antioxidant, antibiofilm, antibacterial, and anticancer effects [18,19]. By raising the intracellular amount of ROS, disrupting the mitochondrial membrane, and inducing programmed cell death against human metastatic ovarian cancer cell lines, the chemical approach showed a potent in vitro cytotoxic effect (HL-60 cells). According to earlier research, the NPs have reportedly demonstrated sound anticancer effects against various cancer cells, including colon, cervical, leukemia, breast, and neuroblastoma [20,21].

Conclusions

The current work covered the environmentally friendly chemistry of producing FeCO₃ nanoparticles by co-precipitating turmeric extract. FeCO₃ nanoparticles' structural properties were examined using FTIR, XRD, and SEM. Studies have revealed that FeCO₃ nanoparticles can inhibit the spread of blood cancer and have potential

therapeutic effects as anticancer agents. FeCO₃ nanoparticles can inhibit the migration and invasion of breast cancer stem cells by raising intracellular ROS levels, rupturing the mitochondrial membrane, and inducing programmed cell death in opposition to them.

References

- [1] Miller, K. D., Siegel, R. L., Lin, C. C., Mariotto, A. B., Kramer, J. L., Rowland, J. H., ... & Jemal, A. (2016). Cancer treatment and survivorship statistics, 2016. CA: a cancer journal for clinicians, 66(4), 271-289.
- [2] Greaves, M. (2016). Leukaemia'firsts' in cancer research and treatment. Nature Reviews Cancer, 16(3), 163-172.
- [3] Alsalem, M. A., Zaidan, A. A., Zaidan, B. B., Hashim, M., Madhloom, H. T., Azeez, N. D., & Alsysisuf, S. (2018). A review of the automated detection and classification of acute leukaemia: Coherent taxonomy, datasets, validation and performance measurements, motivation, open challenges and recommendations. Computer methods and programs in biomedicine, 158, 93-112.
- [4] Sun, M., Lee, J., Chen, Y., & Hoshino, K. (2020). Studies of nanoparticle delivery with

- in vitro bio-engineered microtissues. *Bioactive Materials*, 5(4), 924-937.
- [5] Yen, Y. T., Wang, X., Zhang, H., Wang, C., Lin, Z., Xie, C., ... & Li, R. (2020). Prominent Enhancement of Cisplatin Efficacy with Optimized Methoxy Poly (ethylene glycol)-Polycaprolactone Block Copolymeric Nanoparticles. *Journal of Biomedical Nanotechnology*, 16(3), 335-343.
- [6] Mura, S., & Couvreur, P. (2012). Nanotheranostics for personalized medicine. *Advanced drug delivery reviews*, 64(13), 1394-1416.
- [7] Kalarikkal, N., & Thomas, S. (2020). Challenges in nonparenteral nanomedicine therapy. *Theory and Applications of Nonparenteral Nanomedicines*, 27-54.
- [8] Milto, I. V., Suhodolo, I. V., Prokopieva, V. D., & Klimenteva, T. K. (2016). Molecular and cellular bases of iron metabolism in humans. *Biochemistry (Moscow)*, 81(6), 549-564.
- [9] Torti, S. V., & Torti, F. M. (2020). Iron: The cancer connection. *Molecular aspects of medicine*, 75, 100860.
- [10] Milto, I. V., Suhodolo, I. V., Prokopieva, V. D., & Klimenteva, T. K. (2016). Molecular and cellular bases of iron metabolism in humans. *Biochemistry (Moscow)*, 81(6), 549-564.
- [11] Torti, S. V., & Torti, F. M. (2020). Iron: The cancer connection. *Molecular aspects of medicine*, 75, 100860.
- [12] Anderson, G. J., & Frazer, D. M. (2005, November). Hepatic iron metabolism. In *Seminars in liver disease* (Vol. 25, No. 04, pp. 420-432). Copyright© 2005 by Thieme Medical Publishers, Inc., 333 Seventh Avenue, New York, NY 10001, USA..
- [13] Salah, M., Hammadi, M., Hummadi, E.H.)2021(. Anticancer activity and cytotoxicity of ZnS nanoparticles on MCF-7 human breast cancer cells. *Biochemical and Cellular Archives*, 21(1), pp. 95-99
- [14] Wayne, P. A. (2011). Clinical and laboratory standards institute. Performance standards for antimicrobial susceptibility testing.
- [15] Nassar, M. Y., Ahmed, I. S., Mohamed, T. Y., & Khatab, M. A controlled, template-free, and hydrothermal synthesis route to sphere-like α -Fe₂O₃ nanostructures for textile dye removal.
- [16] Oza, M., & Joshi, M. J. (2017, May). Hydrothermal synthesis of siderite nanoparticles and characterizations. In *AIP Conference Proceedings* (Vol. 1837, No. 1, p. 040037). AIP Publishing LLC.
- [17] Kiss, M. L., Chirita, M., Mihaila, A. I. C., Beljung, C. A., Niznansky, D., & Savii, C. (2015, December). Elucidating some issues regarding the synthesis of superparamagnetic-like single crystalline micrometric Fe₃O₄ during the hydrothermal process. In *AIP Conference Proceedings* (Vol. 1694, No. 1, p. 030006). AIP Publishing LLC.
- [18] Khatami, M., Alijani, H. Q., Fakheri, B., Mobasser, M. M., Heydarpour, M., Farahani, Z. K., & Khan, A. U. (2019). Superparamagnetic iron oxide nanoparticles (SPIONs): Greener synthesis using Stevia plant and evaluation of its antioxidant properties. *Journal of Cleaner Production*, 208, 1171-1177.
- [19] Taghavi, F., Saljooghi, A. S., Gholizadeh, M., & Ramezani, M. (2016). Deferasirox-coated iron oxide nanoparticles as a potential

cytotoxic agent. *MedChemComm*, 7(12), 2290-2298.

- [20] Taghavi, F., Saljooghi, A. S., Gholizadeh, M., & Ramezani, M. (2016). Deferasirox-coated iron oxide nanoparticles as a potential

cytotoxic agent. *MedChemComm*, 7(12), 2290-2298.

- [21] Zhi, D., Yang, T., Yang, J., Fu, S., & Zhang, S. (2020). Targeting strategies for superparamagnetic iron oxide nanoparticles in cancer therapy. *Acta biomaterialia*, 102, 13-34.